# A mechanistic study on SMOB-ADP1: an NADH:flavin oxidoreductase of the two-component styrene monooxygenase of Acinetobacter baylyi ADP1

**ARTICLE** *in* ARCHIVES OF MICROBIOLOGY · AUGUST 2014

Impact Factor: 1.67 · DOI: 10.1007/s00203-014-1022-y · Source: PubMed



**4 AUTHORS**, INCLUDING:

Janosch A. D. Gröning
Technische Universität Bergakademie Frei…
**18** PUBLICATIONS **273** CITATIONS
SEE PROFILE

Stefan R Kaschabek
Technische Universität Bergakademie Frei…
**45** PUBLICATIONS **941** CITATIONS
SEE PROFILE

Dirk Tischler
Technische Universität Bergakademie Frei…
**30** PUBLICATIONS **171** CITATIONS
SEE PROFILE

Arch Microbiol
DOI 10.1007/s00203-014-1022-y

ORIGINAL PAPER

# A mechanistic study on SMOB-ADP1: an NADH:flavin oxidoreductase of the two-component styrene monooxygenase of *Acinetobacter baylyi* ADP1

**Janosch A. D. Gröning · Stefan R. Kaschabek · Michael Schlömann · Dirk Tischler**

Received: 13 June 2014 / Revised: 23 July 2014 / Accepted: 28 July 2014


**Abstract** Two styrene monooxygenase types, StyA/StyB and StyA1/StyA2B, have been described each consisting of an epoxidase and a reductase. A gene fusion which led to the chimeric reductase StyA2B and the occurrence in different phyla are major differences. Identification of SMOA/SMOB-ADP1 of *Acinetobacter baylyi* ADP1 may enlighten the gene fusion event since phylogenetic analysis indicated both proteins to be more related to StyA2B than to StyA/StyB. SMOB-ADP1 is classified like StyB and StyA2B as HpaC-like reductase. Substrate affinity and turnover number of the homo-dimer SMOB-ADP1 were determined for NADH (24 μM, 64 $s^{-1}$) and FAD (4.4 μM, 56 $s^{-1}$). SMOB-ADP1 catalysis follows a random sequential mechanism, and FAD fluorescence is quenched upon binding to SMOB-ADP1 ($K_d$ = 1.8 μM), which clearly distinguishes that reductase from StyB of *Pseudomonas*. In summary, this study confirmes made assumptions and provides phylogenetic and biochemical data for the differentiation of styrene monooxygenase-related flavin reductases.

**Keywords** Styrene monooxygenase · NADH:flavin oxidoreductase · Two-component monooxygenase · Random sequential mechanism · External flavoprotein monooxygenase · HpaC subclass

Communicated by Erko Stackebrandt.

**Electronic supplementary material** The online version of this article (doi:10.1007/s00203-014-1022-y) contains supplementary material, which is available to authorized users.

J. A. D. Gröning · S. R. Kaschabek · M. Schlömann · D. Tischler (✉)
Environmental Microbiology Group, Interdisciplinary Ecological Center, TU Bergakademie Freiberg, Leipziger Str. 29, 09599 Freiberg, Germany
e-mail: dirk-tischler@email.de

## Introduction

NAD(P)H-dependent flavin reductases play a crucial role in conjunction with flavin-dependent monooxygenases (EC 1.13 and EC 1.14) in the catabolism of a multitude of compounds. Styrene monooxygenases (EC 1.14.14.11), catabolic enzymes from styrene metabolism, are a prominent example for flavin-dependent monooxygenases and have been described and characterized from a number of bacteria and yeasts (Montersino et al. 2011; Tischler et al. 2012; Tischler and Kaschabek 2012). According to another classification, they belong to subclass E, a group which covers non-heme, two-component systems, consisting of a flavin reductase and a flavin-dependent monooxygenase (van Berkel et al. 2006). Oxygenation of the vinyl side chain of styrene is performed by the monooxygenase subunit (epoxidase) at the expense of dihydroflavin, which is provided by the NADH-dependent flavin reductase (Fig. 1).

Both enzymes, frequently designated as StyA and StyB, were identified from several pseudomonads (Velasco et al. 1998; Otto et al. 2004; Lin et al. 2010), rhodococci (Toda and Itoh 2012), and *Xanthobacter* (Hartmans et al. 1990) and have been characterized in most detail from *Pseudomonas* sp. VLB120 (Otto et al. 2004) and *P. putida* S12 (Kantz et al. 2005; Kantz and Gassner 2011; Morrison et al. 2013). More recently, the identification of StyA2B from *Rhodococcus opacus* 1CP gave evidence for a remarkable new type of styrene monooxygenase (Tischler et al. 2009). StyA2B constitutes a fusion between the C-terminus of an epoxidase "StyA2" and the N-terminus of a flavin reductase "StyB" and was shown to act as a self-sufficient monooxygenase. However, its oxygenation activity is considerably increased in the presence of an equimolar amount of StyA1 (Tischler et al. 2010). Evidence was provided that despite a tenfold lower specific activity of StyA1/StyA2B (Tischler

Published online: 13 August 2014

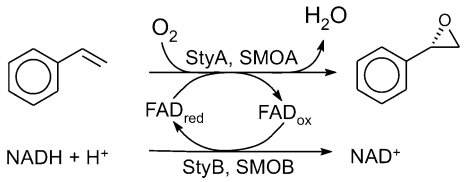


**Fig. 1** Overall reaction of the two-component styrene monooxygenase StyA/StyB from *Pseudomonas* sp.VLB120 and its homolog SMOA/SMOB-ADP1 from *A. baylyi* ADP1. Styrene is epoxidized by StyA or SMOA to (*S*)-styrene oxide at the expense of reduced flavin nucleotides, which become regenerated by NADH-dependent flavin oxidoreductases StyB or SMOB. Both reductive and oxidative half-reaction can be catalyzed by the self-sufficient StyA2B (Tischler et al. 2009)

et al. 2010) compared to the prototype StyA/StyB system from *Pseudomonas* sp. VLB120 (Otto et al. 2004), the transfer of dihydroflavin between the first couple is more specific. A lower degree of uncoupling leads to less oxidative stress and hence to a higher oxygenation efficiency. Very recently, also for StyA/StyB from *Pseudomonas putida* S12, a transient complex formation during catalysis was suggested, which can lead to a more efficient flavin transfer (Morrison et al. 2013). It is therefore not only the epoxidation capacity alone which determines the performance of SMOs but also the specificity of flavin transfer between epoxidase and reductase subunit.

Genome mining for StyA2B-homologs led to the identification of further representatives in the genomes of *R. opacus* MR11, *R. opacus* PD630, *Nocardia farcinica* IFM10152, *Arthrobacter aurescens* TC1, *Variovorax paradoxus* EPS, and *Streptomyces platensis* CR50 (Tischler et al. 2012). However, none of the corresponding proteins have been characterized, so far. Sequence comparison and phylogenetic analysis of identified and hypothetic styrene monooxygenases indicated that the evolutionary appearance of fused SMOs might have happened at least twice (Tischler et al. 2012). Furthermore, the location of a styrene epoxidase (SMOA-ADP1) and flavin reductase (SMOB-ADP1) of *Acinetobacter baylyi* ADP1 within phylogenetic dendrograms indicates that this two-component system is more related to the fused StyA2B of *R. opacus* 1CP than to regular two-component styrene monooxygenase systems of the pseudomonads. This recent identification might represent a kind of missing link or transition between both systems. That SMOA-ADP1 corresponds to a styrene monooxygenase was shown by an initial activity assay in which the monooxygenase converted styrene to styrene oxide (Riedel et al. 2013). How and in particular for what physiological purpose SMOs of type StyA1/StyA2B have been evolved in these bacteria is still unknown.

For the reasons given above, it would be highly interesting to describe SMOB-ADP1 in respect of its reaction mechanism and kinetic parameters and to compare these data with the one of StyB and StyA2B. Such a comparison might enable one to identify and predict correlations between kinetic properties of different flavin reductases and their position within the respective phylogeny. Furthermore, it can provide mechanistic details to further differentiate the two SMOB types (Montersino et al. 2011) for a more precise classification approach, then the two available ones (Lei et al. 1994; Galan et al. 2000).

A first approach classifies these enzymes in respect of the preferred electron donor as FRD-type (preference of NADH), FRP-type (preference of NADPH), and FRG-type flavin reductases (similar activity toward NADH and NADPH) (Lei et al. 1994). Depending on the absence or presence of a tightly bound cofactor, FRD-, FRP-, and FRG-flavoproteins can be further subclassified as class-I- and class-II-flavin reductases, respectively (Tu 2001). They differ also in conserved amino acid motifs, protein fold as well as in the mechanism of the enzymatic reaction (Russell et al. 2004).

A second classification approach divides NAD(P)H:flavin reductases into at least two families and three subfamilies, depending on the usage of flavins as tightly bound prosthetic groups or as substrates (Galan et al. 2000). The family of reductases with tightly bound flavins (flavoproteins) is represented by the Frp reductase of *Vibrio harveyi* (Lei and Tu 1998) and the sulfite reductase of *Escherichia coli* (Covès et al. 1993). The second family consists of at least three subfamilies, of which typological representatives are Fre of *E. coli* (reduction of Fe(III) to Fe(II) at the center of a ribonucleotide reductase), FRase I of *Vibrio fischeri* (coupled luminescence reaction of the luciferase), and HpaC of *E. coli* (degradation of 4-hydroxyphenylacetate) (Galan et al. 2000).

The present paper is dedicated to the putative NAD(P)H:flavin oxidoreductase SMOB-ADP1, which was annotated from the genome of *A. baylyi* ADP1 (BioProject Number PRJNA61597 at NCBI) and which on protein level shows 49 and 72 % of positive positions to StyB (*Pseudomonas* sp. VLB120) and to the reductase part of StyA2B (*R. opacus* 1CP), respectively. Determination of kinetic parameters and reaction mechanism of SMOB-ADP1 allows comparison with both NAD(P)H:flavin oxidoreductases as well as with other reductases from different two-component monooxygenase systems.

## Materials and methods

### Cultivation conditions

*Acinetobacter baylyi* ADP1 was grown at 30 °C on LB plates with 1.5 % (wt/vol) agar. *E. coli* DH5α and strain

BL21 were cultivated for cloning and expression purposes as described somewhere else (Sambrook et al. 2001).

### Cloning of *smo*B-ADP1

The reaction mix for the PCR amplification (100 µl total volume) contained 200 nmol $Mg^{2+}$, 50 pmol of primers ADP1-SMOB-fw (5′-CATATGAATATTAATACATCAC ATG-3′) and ADP1-SMOB-rev (5′-GCGGCCGCTTATGCA CTGAGCTC-3′) (Eurofins MWG Operon), respectively, 32 nmol dNTPs, and 5 U of DreamTaq polymerase (Thermo Fisher Scientific Biosciences). Freshly grown *A. baylyi* ADP1 served as a source of template DNA. The two oligonucleotides contained recognition sites for the restriction endonucleases *Nde*I and *Not*I (underlined sequence) adjacent to the gene-specific sequence (locus_tag ACIAD2674). The amplicon was ligated into the vector pJET1.2 (Thermo Fisher Scientific Biosciences), and the obtained plasmid pJETADP1SMOB was proliferated in *E. coli* DH5α, extracted, and purified. The gene was then excised by *Nde*I-/*Not*I-double digest and ligated into the expression vector pET16bP (U. Wehmeier, personal communication) to yield pETADP1SMOB which was proliferated in *E. coli* DH5α. The amplified and cloned gene was verified by DNA-sequencing (Eurofins MWG Operon). After transformation of pETADP1SMOB into *E. coli* BL21 (DE3) (pLysS), the construct was used for gene expression purposes.

### Expression of $His_{10}$-SMOB-ADP1 in *E. coli* BL21

A preculture of *E. coli* BL21 (pETADP1SMOB) was grown in 15 ml LB-medium (100 µg $ml^{-1}$ ampicillin, 50 µg $ml^{-1}$ chloramphenicol) overnight at 37 °C on a rotary shaker (120 rpm). The complete culture was afterward used to inoculate 1.5 l of 2xYPTG-medium (100 µg $ml^{-1}$ ampicillin, 50 µg $ml^{-1}$ chloramphenicol) in a 2.8-l Fernbach flask. Incubation was continued at 37 °C under constant shaking until an $OD_{600}$ of 0.6 was reached. Induction was initiated by the addition of 1 mM IPTG and further 20 h incubation at 37 °C. Cells were harvested by centrifugation (5,000 × *g*, 15 min, 4 °C) and washed with 54 mM Na/K-phosphate buffer (pH 7.2), and biomass was stored at −80 °C till further use.

### Initial purification, solubilization, and refolding of $His_{10}$-SMOB-ADP1 inclusion bodies

*Escherichia coli* BL21 (pETADP1SMOB) was disrupted by means of a French Press as described elsewhere (Thiel et al. 2005) and centrifuged (5,000 × *g*, 4 °C, 1 h) in order to separate inclusion bodies and soluble protein fraction. For further attempts of purification and renaturation, the obtained pellet containing inclusion bodies was washed twice with sodium phosphate buffer (20 mM, pH 7.5) and stored at −80 °C.

Inclusion bodies were washed and solubilized according to a modified protocol of the QuickFold Protein Refolding Kit (Athena Environmental Sciences, Inc., Baltimore, MD, USA). Instead of deoxycholate, Triton X100 was used in the washing buffer and washing was applied at least 4 times instead of 2 times. The purified inclusion bodies were then stored as aliquots at −80 °C until renaturation. A small portion of homogeneous inclusion bodies was resuspended in 10 µl solubilization buffer (8 M urea, 10 mM DTT, 50 mM Tris–HCl, pH 8.0) per mg pellet and was incubated at 50 °C for 30 min. After centrifugation (20,000 × *g*, room temperature, 30 min), the clear supernatant was adjusted to a protein concentration of 1 mg $ml^{-1}$ (44 µM) or 2 mg $ml^{-1}$ (88 µM) with solubilization buffer. The solubilized protein was then renaturated by drop-wise addition of the protein solution into a 20-fold volume of refolding buffer. The refolding was done twice. At one case, the buffer consisted of 50 mM Tris–HCl (pH 8.0), 240 mM NaCl, 10 mM KCl, 1 mM $Na_2EDTA$, 1 mM reduced glutathione, 0.1 mM oxidized glutathione, and 0.05 % (w/v) PEG 4000. At the other case, the buffer contained additionally 0.1 mM FAD. The refolding mixture was incubated on ice for about 16 h and then subjected directly to a final chromatographic protein purification step. Buffer exchange and concentration steps were achieved by ultrafiltration through a YM10 membrane (regenerated cellulose, NMWL = 10,000 Da, Millipore, USA), which was used within a stirred filtration chamber or as a YM10 Centricon centrifugal filter device. Ammonium sulfate precipitation (80 % saturation) served as an alternative technique for the afore mentioned purposes, but was subsequently omitted due to the observation that the precipitated protein was only partially recoverable.

### Chromatographic protein purification

Protein chromatography was conducted on an ÄKTA fast-performance liquid chromatographer (GE Healthcare).

Anion-exchange chromatography was performed using a MonoQ column (GE Healthcare) and 20 mM Tris–HCl (pH 7.5) as the mobile phase. Elution of bound protein was achieved by means of a linear NaCl gradient (0–1 M), and fractions were subjected to the standard SMOB-ADP1 assay. Fractions with highest flavin reductase activity eluted at approximately 0.3 M NaCl and were pooled for subsequent size-exclusion chromatography.

Nickel-chelate chromatography was used as an alternative purification technique for soluble protein obtained from expression efforts as well as for renaturated $His_{10}$-SMOB-ADP1. For this purpose, 10 ml of cell-free crude extract of *E. coli* BL21 (pETADP1SMOB) or 315 ml of a solution of renaturated $His_{10}$-SMOB-ADP1 (30 mg total protein),

respectively, was applied onto a Ni-Sepharose Fast Flow column (bed volume 26 ml, GE Healthcare), preequilibrated with a buffer of 10 mM Tris–HCl (pH 7.5), 25 mM imidazole, 500 mM NaCl, and 1 mM DTT. Bound $His_{10}$-SMOB-ADP1 was afterward eluted with a linear gradient of imidazole (25–500 mM). Active fractions were pooled.

Size-exclusion chromatography was performed on a Superdex 75 HR-column (30 cm length, 10 mm diameter; GE Healthcare) and 150 mM Tris–HCl (pH 7.5, containing 300 mM NaCl) for size determination or on a Superdex 75 PG-column (60 cm length, 16 mm diameter; GE Healthcare) and 150 mM Tris–HCl (pH 7.5, containing 150 mM NaCl) as the eluent for purification matters.

### Protein quantification and molecular size estimation

Protein concentration was measured according the Bradford method (1976) using the Bradford ULTRA Kit (Expedeon, Cambridge, UK) and bovine serum albumin (BSA) as a calibration standard.

The molecular size of native recombinant $His_{10}$-SMOB-ADP1 was estimated by size-exclusion chromatography as described above. Calibration of the column was done by means of the Gel Filtration Low and High Molecular Weight Calibration Kit (GE Healthcare).

The denatured monomer size of the protein as well as the purity of $His_{10}$-SMOB-ADP1-preparations were determined by discontinuous sodium dodecyl sulfate-polyacrylamide gel electrophoresis (SDS-PAGE) (Sambrook et al. 2001).

### Assay for SMOB-ADP1 activity

The NAD(P)H:flavin oxidoreductase activity was determined spectrophotometrically (Cary WinUV50, Varian) at 25 °C by the consumption of NADH (molar absorption coefficient of 6.22 $mM^{-1}$ $cm^{-1}$) at 340 nm. The standard enzyme assay (1 ml volume) contained 60 nmol FAD and 200 nmol NADH and was buffered with 20 µmol Tris–HCl (pH 7.5). The reaction was started by addition of a suitable amount of enzyme. Kinetic parameters were calculated with the software package KaleidaGraph (version 4.0, Synergy Software, USA) on the assumption that the reactions follow Michaelis–Menten kinetics.

The substrate specificity of the reductase $His_{10}$-SMOB-ADP1 was assayed using the standard assay and sequential exchange of NADH (10.5–217 nmol) by NADPH (150 nmol) as well as of FAD (1.0–98 nmol) by FMN (0.9–130 nmol) and by riboflavin (2.0–143 nmol).

In order to elucidate the order of substrate binding and product release, lumichrome (20 and 60 µM), AMP (1.9 and 3.7 mM), and $NAD^+$ (0.82 and 1.67 mM) were used as competitors for FAD and NADH, respectively. Concentrations of substrate stock solutions were estimated photometrically using the following specific absorption coefficients for lumichrome (10.4 $mM^{-1}$ $cm^{-1}$, 353 nm), AMP (15.4 $mM^{-1}$ $cm^{-1}$, 259 nm), and $NAD^+$ (16.9 $mM^{-1}$ $cm^{-1}$, 259 nm).

Temperature dependence of SMOB-ADP1 activity was determined by means of the standard assay, which was preequilibrated at the respective temperature (between 11 and 52 °C) for 10 min and started by enzyme addition. Determination of the temperature dependence of enzyme stability (between 15 and 54 °C) was carried out slightly modified. After preequilibration for 5 min of an empty vial at the respective temperature, the enzyme was added and incubated for 10 min. After the incubation, the vial with the enzyme was cooled down on ice for 5 min. The enzyme activity was determined by means of the standard assay at 25 °C. Both temperature optima for activity and stability were determined in the presence of 2 mM DTT.

In order to estimate the effect of different buffer systems on SMOB-ADP1-activity, Tris–HCl was substituted in the standard assay by the same amount of MOPS–HCl, TES–NaOH, HEPES–NaOH, imidazol–HCl, and sodium phosphate buffer; all adjusted to a pH of 7.5.

The pH-optimum of $His_{10}$-SMOB-ADP1 was determined by the standard assay in which 100 mM of the following buffers were used: sodium phosphate buffer (pH 5.3, 5.7, 6.2, 6.6, 7.0, 7.5, 8.1, 8.4, 8.8), MOPS–HCl (pH 6.5, 7.5, 7.9), and MES–HCl (pH 5.5, 6.0, 6.5).

Inhibition studies were carried out as described (Tischler et al. 2009). The enzyme assay contained 20 nmol FAD, 20 µmol Tris–HCl (pH 7.5), 400 ng $His_{10}$-SMOB-ADP1, and the particular inhibitor. The assay was then incubated at room temperature for 10 min, and the reaction started by the addition of 160 nmol NADH. The following chemical species were tested: $Ag^+$, $Ca^{2+}$, $Cd^{2+}$, $Cu^{2+}$, $Fe^{2+}$, $Fe^{3+}$, $Hg^{2+}$, $Mg^{2+}$, $Mn^{2+}$, $Ni^{2+}$, $Zn^+$, DTT, $Na_2EDTA$, styrene, styrene oxide, methylphenylsulfide, hydrogen peroxide, mercaptoethanol, sodium azide, *o*-phenanthroline, and iodoacetamide. Metal ions were provided as chlorides, nitrates, and sulfates.

When the reversibility of the inactivation of $His_{10}$-SMOB-ADP1 by $Fe^{2+}$ was assayed, either EDTA or DTT was supplemented to the assay after the protein had been incubated with 0.1 mM $Fe^{2+}$ for 10 min. The assay was then incubated for further 10 min, and the reaction started as described above.

### Fluorescence spectrophotometric analysis

In order to elucidate the interaction of FAD and $His_{10}$-SMOB-ADP1, fluorescence spectra were recorded between 480 nm and 650 nm with a SpectraMax M2*e* (Molecular Devices, USA) (excitation wavelength = 450 nm, cut-off wavelength = 455 nm, PMT gain = 200 V) at 26 °C. The assay (1 ml volume) contained 20 µmol Tris–HCl (pH 7.5), 5.5 nmol FAD, and either 0 or 5 nmol reductase

$His_{10}$-SMOB-ADP1. Every setup was measured two times, and every concentration was measured in duplicate as well.

The dissociation constant ($K_d$) for FAD was determined in a similar way. FAD [10.3 µM stock solution, dissolved in 150 mM NaCl and 150 mM Tris–HCl (pH 7.5)] was titrated against 0.9 ml of buffer [150 mM NaCl and 150 mM Tris–HCl (pH 7.5)] containing appropriate amount of $His_{10}$-SMOB-ADP1. Fluorescence emission was measured at 525 nm with a SpectraMax M2*e* (excitation wavelength = 450 nm, cutoff wavelength = 495 nm, PMT gain = 700 V) at 26 °C. Every assay was measured three times. The fitting of the obtained data was conducted using Eq. 1 (Morrison et al. 2013; Ukaegbu et al. 2010).

$$F = \varepsilon_1 * [\text{FAD}]_{\text{total}} + ((K_d^{\text{app}} + [\text{FAD}]_{\text{total}} + [\text{SMOB - ADP1}]_{\text{total}}) - ((K_d^{\text{app}} + [\text{FAD}]_{\text{total}} + [\text{SMOB - ADP1}]_{\text{total}})^2 - 4 * [\text{FAD}]_{\text{total}} * [\text{SMOB - ADP1}]_{\text{total}})^{1/2})/2 * (\varepsilon_2 - \varepsilon_1) \quad (1)$$

To determine the fluorescence emission of free, oxidized FAD in the used buffer, a similar titration experiment was carried out, but omitting $His_{10}$-SMOB-ADP1.

For the determination of the dissociation constant of FAD, the $His_{10}$-SMOB-ADP1 preparation was used, which had been refolded in the presence of FAD. Though the refolded protein was applied to a size-exclusion chromatography, the sample contained still some FAD. The FAD concentration in the sample was determined by measuring the absorption at 450 nm and considered in later data analysis.

### Bioinformatic analysis

Multiple sequence alignment of amino acid sequences of flavin reductases was done with the program ClustalX (version 2.1) (Thompson et al. 1997). PHYLIP 3.69 (Felsenstein 1989) served as software for distance matrix calculation, and embedded tools PROTDIST and FITCH were used with default settings. The resulting treefile was evaluated using Seaview (version 4.3.1) (Gouy et al. 2010).

BLASTX and BLASTP (Altschul et al. 1990) were used for sequence analysis within the non-redundant protein database NCBI.

## Results and discussion

### SMOA-ADP1 and SMOB-ADP1 constitute unique branches that root between the phylogenetic clades of classical two-component SMOs and fused SMO-homologs

Based on their sequence, mechanism, and structure, flavin-dependent styrene monooxygenases can be classified into two-component styrene monooxygenases of type StyA/StyB (reported from *Pseudomonas* sp. VLB120 (Otto et al. 2004), *P. fluorescens* ST (Beltrametti et al. 1997), and *Rhodococcus* sp. ST-5 and ST-10 (Toda and Itoh 2012) and fused SMOs of type StyA2B (reported from *R. opacus* 1CP (Tischler et al. 2009), *Rhodococcus* sp. MR11 (Tischler et al. 2012), *V. paradoxus* EPS, *S. platensis* CR50, *A. aurescens* TC1, and *N. farcinica* IFM10152 (Tischler et al. 2012; van Hellemond et al. 2008). At first, both groups of proteins can be distinguished in respect of the presence or absence of an additionally fused oxygenase variant at the N-terminus of the reductase. Secondly, the genetic location differs considerably, and genes of classical two-component styrene monooxygenases are typically part of styrene-catabolic operons (Velasco et al. 1998; Panke et al. 1998; O'Leary et al. 2001). Thirdly, this gets obvious by phylogenetic analysis, oxygenase as well as reductase subunits of both groups form single clades within a dendrogram (Tischler et al. 2012). A recent expansion of available sequences within these dendrograms led to the identification of two adjacent genes from the genome of *A. baylyi* ADP1, which according to conceptual translation encode a putative monooxygenase (ACIAD2675) and a reductase (ACIAD2674). Interestingly, the corresponding proteins, designated as SMOA-ADP1 and SMOB-ADP1, were both found to form independent branches, which root between the clades of both groups (exemplary shown for reductases, Fig. 2). It should be mentioned that styrene-epoxidizing activity of recombinant SMOA-ADP1 was recently verified by experimental evidence (Riedel et al. 2013). Furthermore, the neighboring region of *smoA*/*smoB*-ADP1 does not encode styrene-catabolic enzymes such as styrene oxide isomerase StyC and phenylacetaldehyde dehydrogenase StyD, as it is often the case for classical two-component SMOs. Instead, a gene encoding a putative short-chain dehydrogenase is located upstream of *smoA*-ADP1. Together with a putative dienelactone hydrolase-encoding gene, this topology was reported for the class of SMOs of type StyA1/StyA2B (Tischler et al. 2012).

### SMOB-ADP1 belongs to flavin reductases of the HpaC-like subfamily

In order to align SMOB-ADP1 of *A. baylyi* ADP1 to known NAD(P)H:flavin oxidoreductases and hence to classify it according to Galan et al. (2000), a multiple amino acid sequence alignment was conducted with different representatives of known families. SMOB-ADP1 turned out to exhibit basically the same conserved regions as members of the HpaC-like subfamily are characterized by (Fig. 3). Flavin reductases of the HpaC-like subfamily, for which Galan and co-workers identified a 4-hydroxyphenylacetate 3-monooxygenase of *E. coli* W as the prototype, can be

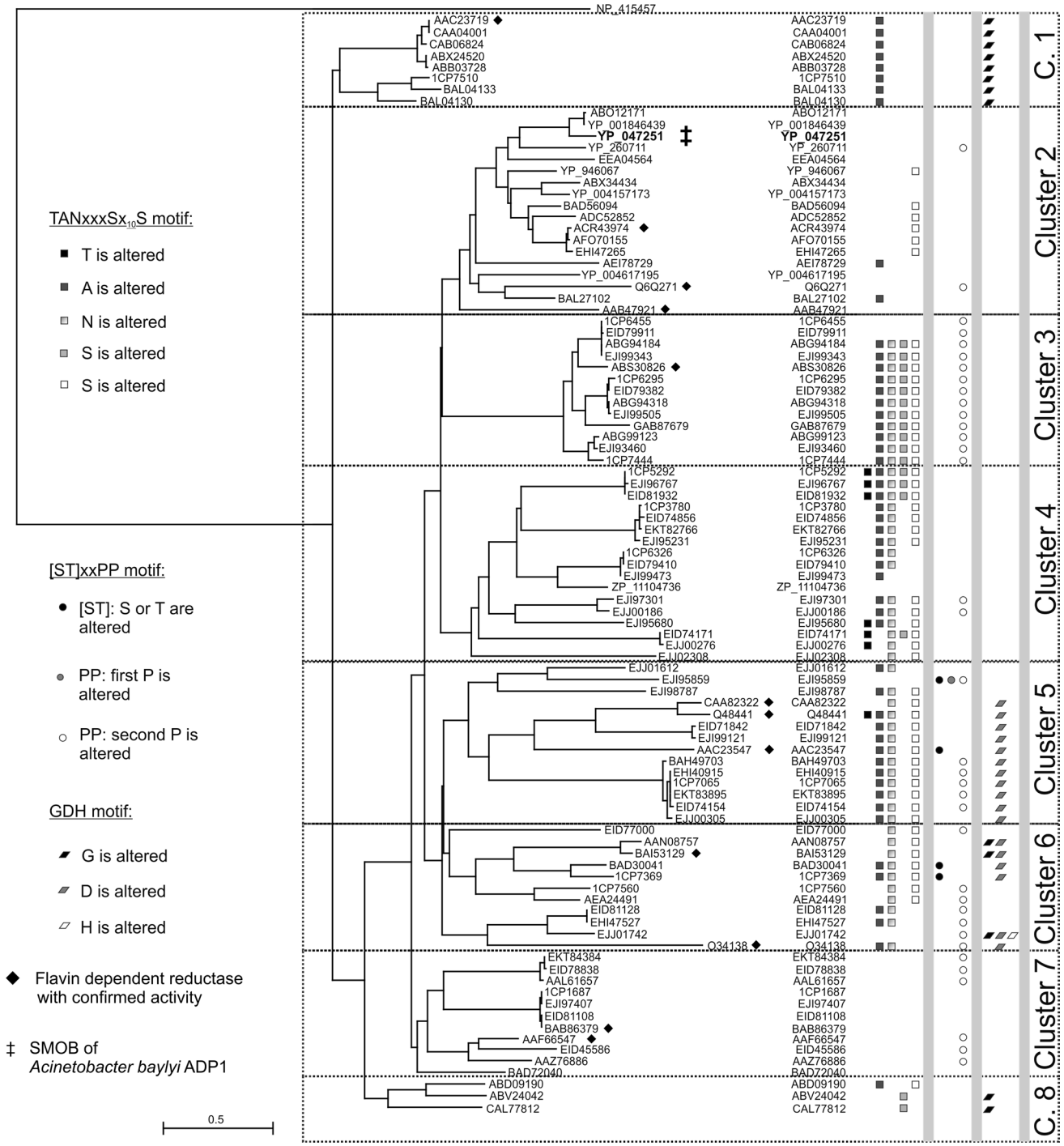


**Fig. 2** Dendrogram of putative and experimentally confirmed NAD(P)H-dependent flavin oxidoreductases (see also Table 2). The dendrogram was calculated by means of ClustalX (version 2.1), GeneDoc (version 2.6.003), and the moduls PROTDIST and FITCH of the PHYLIP package (version 3.69), and NCBI protein accession numbers are given. Amino acid sequences of fused flavin oxidoreductases StyA2B were truncated for their N-terminal monooxygenase part. Accession numbers starting with "1CP" refer to amino acid sequences from an unpublished genome sequencing project. The NAD(P)H-dependent FMN reductase of *E. coli* str. K-12 substr. MG1655 (NP_415457) was used as outgroup

identified by two amino acid motifs. A residue of Ser (Thr or Cys) located before a pair of conserved proline residues is highly conserved at the N-terminus of proteins, whereas the consecutive residues Gly, Asp, and His are typical for the C-terminus (Galan et al. 2000; van Lanen et al. 2009). The latter residues are discussed as a pyridine nucleotide

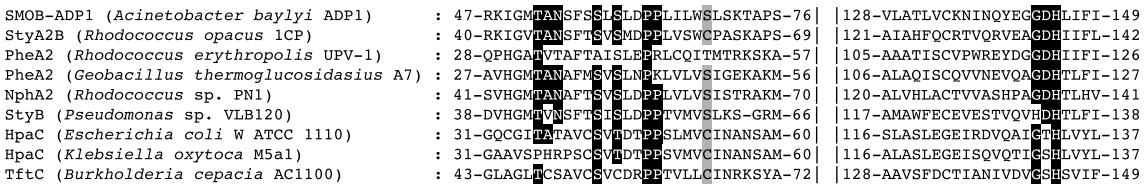


**Fig. 3** Multiple protein sequence alignment of representatives of the HpaC-like subfamily belonging to flavin oxidoreductases with confirmed activity (Galan et al. 2000). Highly conserved motifs of this subclass presented in the phylogenetic tree (Fig. 2) are *shaded black* and *gray*. Protein designations and accession numbers are as follows: SMOB-ADP1 of *A. baylyi* ADP1 (YP_047251), StyA2B of *R. opacus* 1CP (ACR43974) truncated for its N-terminal monooxygenase region, PheA2 of *R. erythropolis* UPV-1 (ABS30826), PheA2 of *G. thermoglucosidasius* A7 (AAF66547), NphA2 of *Rhodococcus* sp. PN1 (BAB86379), StyB of *Pseudomonas* sp. VLB120 (AAC23719), HpaC of *E. coli* W ATCC 1110 (CAA82322), HpaC of *Klebsiella oxytoca* M5a1 (Q48441), TftC of *Burkholderia cepacia* AC1100 (AAC23547). All protein sequences are truncated to the region of the relevant motifs. Amino acid positions of all proteins are indicated

interaction motif, and histidine likely plays a crucial role in NADH binding as shown by Russell and co-workers by mutational analysis of the NADH:flavin oxidoreductase ($FRD_{Aa}$) of *Aminobacter aminovorans* (Russell and Tu 2004).

Both motifs, "[STC]xxPP" and "GDH," could be also identified in SMOB-ADP1 of *A. baylyi* ADP1 and hence allow classification of SMOB-ADP1 into the HpaC-like subfamily. The biochemical data obtained strengthen this classification since FAD serves rather as a substrate than a prosthetic group.

A third conserved sequence motif described by Thotsaporn et al. (2004) could be identified close to the N-terminus of SMOB-ADP1. It is constituted by the sequence TANxxSx10S and is supposed to play a crucial role in the interaction with isoalloxazine and NADH.

In all of the protein sequences which were used to calculate the dendrogram (Fig. 2; for multiple protein sequence alignment, see supplementary material Fig. S2), the afore mentioned three sequence motifs could be identified to some extent. It is strikingly obvious that the clusters can be separated by the variations of amino acids in the three conserved motifs and that the changes are quite consistent within a single cluster.

The phylogenetic relatedness between NAD(P)H:flavin oxidoreductases is widely reflected by the corresponding monooxygenase moieties, since the latter one yield a similar clustering in the dendrogram (Tischler et al. 2012). This is a strong evidence for coevolution. Oxygenases and reductases of two-compound monooxygenases obviously have not been exchanged during evolution. Such a strong conservation and dependency from each other could indicate a specific and important form of interaction, which should be responsible for the transfer of reduced FAD from the oxidoreductase to the oxygenase moiety. Although some oxygenases have shown to utilize reduced FAD provided by electrochemical preparation or by the activity of only distinctly related flavin reductases, obtained oxygenation rates were either lower or the transfer process was less efficient when compared with the original oxidoreductases (Tischler et al. 2010; Hollmann et al. 2003).

## Cloning, expression, and refolding of $His_{10}$-SMOB-ADP1

On basis of the available genome sequence of *A. baylyi* ADP1 (CR543861), two oligonucleotides ADP1-SMOB-fw and ADP1-SMOB-rev were designed and allowed the amplification of the complete gene *smoB*-ADP1 (~ 550-bp). After ligation into the cloning vector pJET1.2, confirmation by DNA-sequencing, and excision by *Nde*I/*Not*I-double digest, *smoB*-ADP1 was transferred into the expression vector pET16bP.

After transformation of the obtained plasmid pETADP1SMOB into *E. coli* BL21, expression of the $His_{10}$-tagged protein was induced in the presence of IPTG. The formation of $His_{10}$-SMOB-ADP1 became apparent during SDS-PAGE by an intense band between 20 and 25 kDa, which corresponded roughly to the calculated size of 22,665 Da (data not shown). However, analysis of the soluble and the insoluble fraction of induced biomass indicated the predominant formation of inclusion bodies. Minor amounts of the soluble active protein could only be obtained, when induction was performed at room temperature but were insufficient for a more detailed kinetic enzyme characterization.

As a consequence, and similar to recombinantly expressed StyB of *Pseudomonas* sp. strain VLB120 (Otto et al. 2004), obtained inclusion bodies were purified, solubilized, and successfully renaturated. Application of the modified renaturation buffer no. 12 of the commercial QuickFold Protein Refolding Kit (Athena Environmental Sciences, Inc., Baltimore, MD, USA), consisting of 50 mM Tris–HCl (pH 8.0), 240 mM NaCl, 10 mM KCl, 1 mM $Na_2EDTA$, 1 mM reduced glutathione, 0.1 mM oxidized glutathione, and 0.05 % (w/v) PEG 4000, yielded a specific reductase activity of approx. 100 U $mg^{-1}$, no matter whether FAD was added or omitted in the refolding buffer.

For subsequent fluorescence measurements (refolding without FAD for observation of the quenching effect of FAD and refolding with FAD for the binding studies of $His_{10}$-SMOB-ADP1 and FAD), native molecular size estimation (refolding without FAD), inhibition studies with $NAD^+$ (refolding without FAD), determination of kinetic parameters and kinetic mechanism (refolding with FAD), and temperature stability (refolding with FAD) refolded $His_{10}$-SMOB-ADP1 was subjected to ultrafiltration (NMWL = 3,000 Da) and MonoQ-chromatography, during which oxidoreductase eluted as a single protein peak at 300 mM NaCl. The purified protein had a specific activity of 115 U $mg^{-1}$ while being refolded without addition of FAD (NADH = 156 µM; FAD = 49 µM) or 110 U $mg^{-1}$ when the refolding was done in the presence of FAD (NADH = 200 µM; FAD = 51 µM). These two specific activities for the refolded $His_{10}$-SMOB-ADP1 were about as high as described for recombinant StyB from strain VLB120 (200 U $mg^{-1}$) (Otto et al. 2004). The result indicated a successful renaturing of $His_{10}$-SMOB-ADP1 and gave no obvious evidence for a negative effect of the N-terminal histidine tag on activity.

The purified oxidoreductase $His_{10}$-SMOB-ADP1, regardless of been expressed in active form or renaturated from inclusion bodies, was colorless, and the UV spectrum gave no evidence for a covalently bound flavin residue or another chromogenic cofactor (data not shown). This property is consistent with the proposed classification of SMOB-ADP1 into the HpaC-like subfamily.

Denaturing high-resolving SDS-PAGE analysis of homogeneous $His_{10}$-SMOB-ADP1 yielded a single band at the size of approximately 22 kDa (data not shown). Taking into account the retention behavior of the refolded native apo-$His_{10}$-SMOB-ADP1 during size-exclusion chromatography which corresponds to a native weight of around 41 kDa, the quaternary structure is likely to be that of a homo-dimer. Other reductases of classical two-component monooxygenases often appear as homo-dimeric entities, too, such as StyB of *Pseudomonas* sp. strain VLB120 (Otto et al. 2004), HpaC of *E. coli* W (Galan et al. 2000), $FRD_{Aa}$ of *A. aminovorans* ATCC 29600 (Russell et al. 2004), and PheA2 of *Geobacillus thermoglucosidasius* A7 (Kirchner et al. 2003).

## SMOB-ADP1 represents an NADH-specific flavin oxidoreductase

SMOB-ADP1-activity of the homogeneous His-tagged protein was shown to be solely dependent on the presence of NADH and FAD within the assay. Neither SMOA-ADP1, nor styrene or any other cofactor was necessary. The specificity of SMOB-ADP1 toward the electron-donating substrate NADH was shown to be strict since the phosphorylated analog NADPH yielded no measurable activity. The Michaelis–Menten constant $K_{m,NADH}$ and turnover number $k_{cat,NADH}$ in the presence of FAD were determined to be 24 ± 2.8 µM and 64 ± 1.9 $s^{-1}$ (Fig. S1). A much higher tolerance of SMOB-ADP1 was measured toward flavin-containing electron acceptors. On the basis of catalytic efficiency $k_{cat}\ K_m^{-1}$, they are preferred in the order FAD (3.6 $\mu M^{-1}\ s^{-1}$) > riboflavin (1.9 $\mu M^{-1}\ s^{-1}$) ≥ FMN (1.4 $\mu M^{-1}\ s^{-1}$) but the overall variation never exceeds factor 3 (Table 1). This low specificity is also reflected by the substrate affinities ($K_m$) of $His_{10}$-SMOB-ADP1 toward FAD (4.2 ± 0.46 µM), FMN (5.5 ± 0.29 µM), and riboflavin (11 ± 0.6 µM) (Table 2).

The exclusive utilization of the electron donor NADH by SMOB-ADP1 is a property shared with the fused flavin reductase StyA2B of *R. opacus* 1CP and StyB of *Pseudomonas* sp. VLB120 (Table 1).

As shown in Table 1, the Michaelis–Menten constant $K_{m,FAD}$ does not differ significantly between the initial measurements of the soluble expressed $His_{10}$-SMOB-ADP1 and the latter used insoluble expressed and refolded $His_{10}$-SMOB-ADP1 protein preparation. By this observation, we concluded that the refolding itself has probably no influence on the biochemical properties of the protein.

Galan et al. (2000) could measure a reductase activity for the HpaC-prototype from *E. coli* W with NADPH. However, since the observed specific activities were diminished by a factor of approximately 100 compared to NADH, the non-phosphorylated cofactor is the preferred electron-donating substrate for HpaC-like reductases of two-component monooxygenases.

The affinity of $His_{10}$-SMOB-ADP1 toward the flavin-containing substrate FAD exceeds that to NADH by a factor of approximately 5, a behavior which is shared by the protein HpaC of *E. coli* W. The two other compared flavin reductases StyA2B (*R. opacus* 1CP) and StyB (*Pseudomonas* sp. VLB120) exhibit only a twofold higher affinity to FAD.

The catalytic efficiencies of the two-component system flavin oxidoreductases SMOB-ADP1, StyB, and HpaC are in the same range of order. Compared to these values, the flavin oxidoreductase of the fused StyA2B-system exhibits a 10- to 100-fold lower catalytic efficiency toward FAD and NADH.

The temperature optimum of $His_{10}$-SMOB-ADP1-activity was determined to be 44 ± 3 °C (see Fig. 4). However, incubation of the enzyme at this temperature for 10 min was accompanied with a loss of around 35 % of the activity. Within that period temperatures above 40 °C led to a significant decrease of activity. The SMOB-ADP1 temperature stability fits well to the optimal growth conditions for strain ADP1 (Metzgar et al. 2004).

**Table 1** Overview of available kinetic parameter obtained for NAD(P)H:flavin oxidoreductases

| Enzyme (source) | Substrate (cosubstrate) | $K_m$ (μM) | $k_{cat}$ ($s^{-1}$) | $k_{cat} K_m^{-1}$ ($s^{-1}$ $\mu M^{-1}$) | References |
|---|---|---|---|---|---|
| $His_{10}$-SMOB-ADP1 (*A. baylyi* ADP1) | NADH (FAD) | 24 ± 2.8 | 64 ± 1.9 | 2.7 ± 0.41 | This study |
| | NADPH (FAD) | n. d. | 0 | n. d. | |
| | FAD (NADH) | 4.4 ± 0.31 | 56 ± 0.90 | 13 ± 1.2 | |
| | FAD (NADH) | 4.2 ± 0.46[a] | 15 ± 0.4[a] | 3.6[a] ± 0.51 | |
| | FMN (NADH) | 5.5 ± 0.29[a] | 7.8 ± 0.12[a] | 1.4[a] ± 0.098 | |
| | Riboflavin (NADH) | 11 ± 0.6[a] | 21 ± 0.4[a] | 1.9[a] ± 0.13 | |
| StyB (*Pseudomonas* sp. VLB120) | NADH (FMN) | 21.06 ± 2.6 | 60 | 2.84 | Otto et al. (2004) |
| | NADPH | No activity | No activity | No activity | |
| | FAD (NADH) | 11.6 ± 1.4 | 47 | 4.05 | |
| | FMN (NADH) | 7.1 ± 0.7 | 48 | 6.78 | |
| | Riboflavin (NADH) | 14.7 ± 2.8 | 60 | 4.08 | |
| $His_{10}$-StyA2B (*R. opacus* 1CP) | NADH (FAD) | 58 ± 9 | 3.9 ± 0.3 | 0.068 | Tischler et al. (2009) |
| | NADPH (FAD) | n. d. | <0.01 | n. d. | |
| | FAD (NADH) | 26 ± 2 | 5.2 ± 0.2 | 0.203 | |
| | FMN (NADH) | 67 ± 22 | 4.8 ± 1.0 | 0.071 | |
| | Riboflavin (NADH) | 23 ± 2 | 3.0 ± 0.1 | 0.131 | |
| HpaC (*E. coli* W) | NADH (FMN) | 40 | n. d. | n. d. | Galan et al. (2000) |
| | NADPH | n. d. | 2 magnitudes lower than with NADH | n. d. | |
| | FAD (NADH) | 3.1 | 11[b] | 3.5 | |
| | FMN (NADH) | 2.1 | 21[b] | 10 | |
| | Riboflavin (NADH) | 2.6 | 18[b] | 6.9 | |

*n. d.* not determined

[a] Soluble expressed and enriched $His_{10}$-SMOB-ADP1

[b] $k_{cat}$ was calculated from $v_{max}$ (Galan et al. 2000) using the molecular weight of 18,679 Da (Prieto and Garcia 1994) for one catalytically active subunit

**Table 2** The functional identity of flavin reductases with confirmed activity used in the dendrogram (Fig. 2)

| Accession number | Organism | Name | References |
|---|---|---|---|
| AAB47921 | *Aminobacter aminovorans* ATCC 29600 | NADH:flavin oxidoreductase ($FRD_{Aa}$) | Russell et al. (2004) |
| AAC23547 | *Burkholderia cepacia* AC1100 | Chlorophenol-4-monooxygenase, component 1 (TftC) | Gisi and Xun (2003) |
| AAC23719 | *Pseudomonas* sp. VLB120 | Styrene monooxygenase, small component (StyB) | Otto et al. (2004) |
| AAF66547 | *Geobacillus thermoglucosidasius* A7 | Phenol 2-hydroxylase, component B (PheA2) | Kirchner et al. (2003) |
| ABS30826 | *Rhodococcus erythropolis* UPV-1 | Phenol hydroxylase, small subunit (PheA2) | Saa et al. (2010) |
| ACR43974 | *Rhodococcus opacus* 1CP | Styrene monooxygenase, reductase component (StyA2B)[a] | Tischler et al. (2009) |
| BAB86379 | *Rhodococcus* sp. PN1 | 4-Nitrophenol hydroxylase, component B (NphA2) | Takeo et al. (2008) |
| BAI53129 | *Arthrobacter* sp. IF1 | 4-Fluorophenol monooxygenase, reductase component (FpdB) | Ferreira et al. (2009) |
| CAA82322 | *Escherichia coli* ATCC 1110 | 4-Hydroxyphenylacetate 3-monooxygenase, reductase subunit (HpaC) | Galan et al. (2000) |
| O34138 | *Streptomyces viridifaciens* MG456-hF10 | Isobutylamine hydroxylase, flavin reductase component (VlmR) | Parry and Li (1997) |
| Q48441 | *Klebsiella oxytoca* M5a1 | 4-Hydroxyphenylacetate 3-monooxygenase, reductase component (HpaC) | Gibello et al. (1997) |
| Q6Q271 | *Acinetobacter baumannii* | *p*-Hydroxyphenylacetate 3-hydroxylase, reductase component (C1-HpaH) | Chaiyen et al. (2001) |
| YP_047251 | *Acinetobacter baylyi* ADP1 | Styrene monooxygenase, NADH:flavin oxidoreductase component (SMOB-ADP1) | This study |

[a] Amino acid sequences of fused flavin oxidoreductases StyA2B were truncated for their N-terminal monooxygenase part

The pH-optimum of reductase activity was determined in the range of 6.3–7.5. A similar activity plateau between around 6.2 and 8.7 was reported for the NADH:flavin oxidoreductase PrnF from *Pseudomonas fluorescens* Pf-5 (Tiwari et al. 2012). Beyond this range, $His_{10}$-SMOB-ADP1 turned out to be especially susceptible against acidic conditions. Activity irreversibly dropped to under 5 % at pH 5.3 indicating denaturation. From the investigated buffer systems, only K/Na-phosphate and imidazole–HCl affected $His_{10}$-SMOB-ADP1 in a significant extent, leading to a 10 % decrease and increase, respectively, at pH 7.5. Chloride seemed not to have a negative effect on $His_{10}$-SMOB-ADP1 activity as there was no difference in the activity when assayed with Tris–HCl or TES–NaOH. This insensitivity toward chloride is shared by StyA2B of *R. opacus* 1CP (Tischler et al. 2009).

## FAD-reduction by $His_{10}$-SMOB-ADP1 follows a random sequential mechanism

An enzymatic reaction which converts two substrates into two products can follow either a sequential bisubstrate–biproduct (Bi Bi) or a ping-pong Bi Bi mechanism. In order to distinguish both kinetics, the reciprocal initial velocities can be plotted versus the reciprocal substrate concentrations according to Lineweaver–Burk yielding either a set of parallel or intersecting lines, respectively. Though the lowest NADH concentration at varied FAD concentration (Fig. 5a) might suggest some ping-pong kinetics, the overall observation for the two sets of experiments, varying FAD concentrations at four different NADH concentrations (161, 115, 77, 39 µM) and varying NADH concentrations at four different FAD concentrations (82, 51, 36, 20 µM), resulted in both cases in intersecting lines (Fig. 5). This observation strongly suggests a sequential mechanism and implies that only free FAD takes part in the enzymatic reaction instead of protein-bound FAD. That is in congruence with the enrichment of soluble SMOB-ADP1 since no protein-bound or tightly interacting FAD was observed.

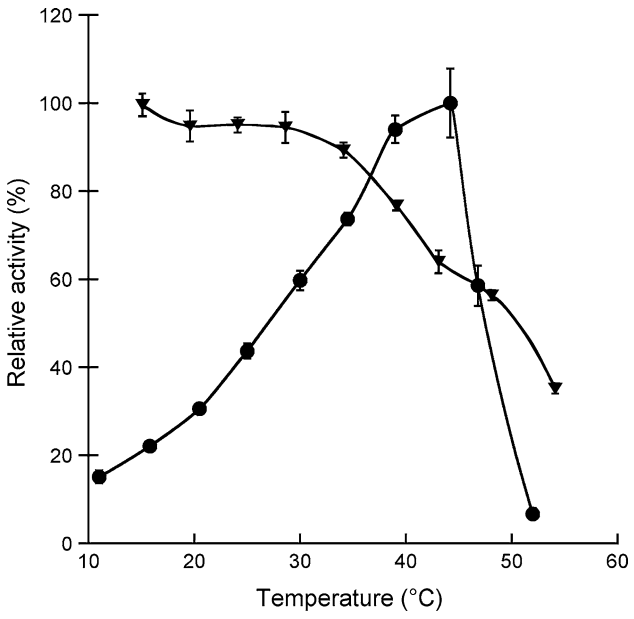


**Fig. 4** Effect of temperature on the specific activity (*circles*; 100 % relative activity refers to a specific activity of 147 ± 12 U $mg^{-1}$) and the stability (*triangles*; 100 % relative activity refers to a specific activity of 95 ± 2.5 U $mg^{-1}$) of the flavin oxidoreductase SMOB-ADP1. Each data point results from three independent measurements. Enzyme stability was determined by measuring the residual specific activity at 25 °C after 10 min of incubation at the corresponding temperature, whereas the temperature dependence of specific activity was measured without thermal pretreatment of SMOB-ADP1

The sequential-type of substrate binding at an enzyme can be either of random or of ordered nature (Fromm 1979; Russell et al. 2004). In order to distinguish between both mechanisms, inhibition studies were conducted using the dead-end inhibitors AMP and lumichrome. When lumichrome was present at constant FAD level and NADH was varied, the measured $K_{m,app}$ for NADH remained constant (≈ 23 µM) and *kcat* decreased substantially (−33 %), indicating a noncompetitive inhibition type. As expected, these data suggest that lumichrome does neither interact with the binding site for NADH nor otherwise interferes in the binding process of the electron donor. However, a slowed down reaction rate indicates an interference with the second substrate FAD. In fact, a 3.5-fold increase of $K_{m,app,FAD}$ was determined in the presence of lumichrome, when FAD concentrations were varied at constant NADH level. Simultaneously, the turnover number decreased for about 45 %. Thus, a mixed noncompetitive inhibition is very likely and suggests that the binding of the inhibitor is favored when the enzyme–substrate complex has already been formed. The mixed noncompetitive inhibition of FAD-binding of SMOB-ADP1 by lumichrome differs from that one of the reductase $FRD_{Aa}$ of *A. aminovorans* ATCC 29600 (Russell et al. 2004), which was shown to be competitive.

When AMP was applied as a potential inhibitor and NADH was varied at constant FAD level, the $K_{m,app}$ increased from 16 ± 1.1 to 31 ± 1.9 µM. In addition, the maximum reaction rate (61.2 ± 1.0 U $mg^{-1}$) increased for about 20 % demonstrating a mixed noncompetitive inhibition. These results indicate that AMP can bind to the binding site of NADH as well as to another site, which is proposed to be the binding site of FAD. The latter assumption is based on the fact that an AMP-moiety is a common part of both substrates, NADH and FAD. Binding to both sites results in a mixed inhibition since AMP then may bind to apo-SMOB-ADP1, to FAD-SMOB-ADP1, or to NADH-SMOB-ADP1 effecting binding and second-order reaction rate.

A competitive inhibition of SMOB-ADP1 by AMP resulted toward the substrate FAD. Decreasing the FAD concentration at constant NADH level led to an increase of $K_{m,app,FAD}$ from 3.7 ± 0.3 to 6.0 ± 0.5 µM, whereas $k_{cat}$ remained almost constant (27 ± 0.5–28 ± 0.6 $s^{-1}$). The calculated $K_i$ value for AMP is 6.6 ± 4.4 mM. The possible binding of AMP to the FAD-binding site was already suggested and herewith confirmed. In case of this competitive inhibition of FAD-binding to apo-SMOB-ADP1 or NADH-SMOB-ADP1, it becomes clear that AMP can solely bind to the protein and not to the protein-FAD complex indicating a stronger affinity of SMOB-ADP1 for FAD.

Based on the observed inhibition types for lumichrome and AMP, we propose a random mechanism for the binding of the substrates NADH and FAD. That conclusion suggests itself in particular from lumichrome inhibition experiments, since in case of varied NADH concentration, lumichrome caused a noncompetitive inhibition pattern. It means lumichrome binds to SMOB-ADP1 unaffected if NADH has already bound or not. In addition, no evidence was provided that FAD has to bind to SMOB-ADP1 as the first substrate. That clearly differentiates SMOB-ADP1 of strain ADP1 from StyB of *Pseudomonas* sp. VLB120 and SMOB of *P. putida* S12 for which both an ordered binding mechanism with NADH as leading substrate was reported (Otto et al. 2004; Kantz et al. 2005). In the latter case, an uncompetitive inhibition by lumichrome can be expected as shown for other reductases (Russell et al. 2004).

Similar to the binding of substrate, product release can be classified as random- or ordered type. For the purpose of differentiation, the product $NAD^+$ was used as a competitor in different concentrations (Rudolph 1979). Variation of NADH at fixed FAD level and reverse both resulted in a mixed-type inhibition (Fig. 6) and indicated a random mechanism of $NAD^+$ and FADred product release. Like substrate binding, product release of SMOB-ADP1 differs to the one of StyB for which $NAD^+$ is supposed to block the desorption of FADred. Hence, $NAD^+$ leaves the active site prior to FADred, which afterward migrates to StyA for epoxidation process (Morrison et al. 2013).

### NADH:flavin oxidoreductases SMOB-ADP1 and StyB of two-component styrene monooxygenases share a pronounced sensitivity toward ferrous iron

Incubation of SMOB-ADP1 with different potential inhibitors may give hints on functionally or structurally relevant residues and prosthetic groups/cofactors. Not surprisingly, thiol-reactive heavy metals, such as $Ag^+$ (19 % residual SMOB-ADP1 activity), $Cu^{2+}$ (25 %), $Hg^{2+}$ (40 %) and $Cd^{2+}$ (43 %), showed a drastic impact between 10 and 20 µmol $l^{-1}$. However, oxidation of the amino acid cysteine may not be the only cause for denaturation here since SMOB-ADP1 was found to be resistant toward hydrogen peroxide. About 100 µM of this strong oxidant did not show any effect and even at concentrations of about 50 mM only one-tenth of activity got lost. The resistance of $His_{10}$-SMOB-ADP1 toward the alkylating agent iodoacetamide indicates that thiol groups are either not freely accessible or not involved in reaction mechanism.

Chelating compounds such as EDTA and *o*-phenanthroline which act on a number of metal ions did not deplete SMOB-ADP1 activity indicating dispensability of the latter ones and especially that of a heme group. A lack of inactivation was also noticed for sodium azide (500 µM), which otherwise interferes in the center of metalloenzymes. Instead, the addition of 10 mM $Na_2EDTA$ or 500 µM sodium azide led to a significant increase of SMOB-ADP1-activity (44 and 18 %, respectively). This effect is likely caused by the elimination of traces of $Ni^{2+}$-ions being leached during IMAC of the recombinant His-tagged protein. In fact, 100 µM $Ni^{2+}$ was shown to yield a significant 30 % decrease in SMOB-ADP1 activity. Similar to EDTA, a $Ni^{2+}$-masking mechanism may be responsible for the positive effects of DTT and mercaptoethanol, which both slightly increased SMOB-ADP1-activity. The reducing effect of these agents which prevents cysteine residues from oxidation is probably not responsible for this behavior because of the afore mentioned insensitivity of SMOB-ADP1 toward $H_2O_2$. Since these reducing agents are also able to break structurally essential disulfide bridges, the results indicate that those structures are at least not present at the accessible surface of the protein.

Incubation of $His_{10}$-SMOB-ADP1 with different metals of the iron group ($Ni^{2+}$, $Mn^{2+}$, $Fe^{2+/3+}$) pointed to a particular susceptibility toward $Fe^{2+}$. About 100 µM ferrous iron completely abolished reductase activity while manganese as well as ferric iron showed no or only minor effects, respectively. Simultaneous presence of 10 mM EDTA diminished the action of 100 µM $Fe^{2+}$ up to an overall decrease of 38 % activity. A comparable susceptibility toward ferrous iron could be determined in this study for StyB from *Pseudomonas* sp. VLB120 which in presence of 100 µM $Fe^{2+}$ lost 84 % of its initial activity (Fig. 7c). Interestingly, this behavior seems not to be typical for oxidoreductases of the fused type since StyA2B of *R. opacus* 1CP turned out to be unaffected.

Substrates and products of the flavin-dependent monooxygenase subunit StyA may represent other potential inhibitors and were tested, too. Styrene, styrene oxide, methyl phenylsulfoxide, and thioanisole—the latter two are not of physiological relevance—as well as the afore mentioned hydrogen peroxide as a by-product of FADred autooxidation (Massey 1994) showed almost no or only marginal effects at the tested concentrations.

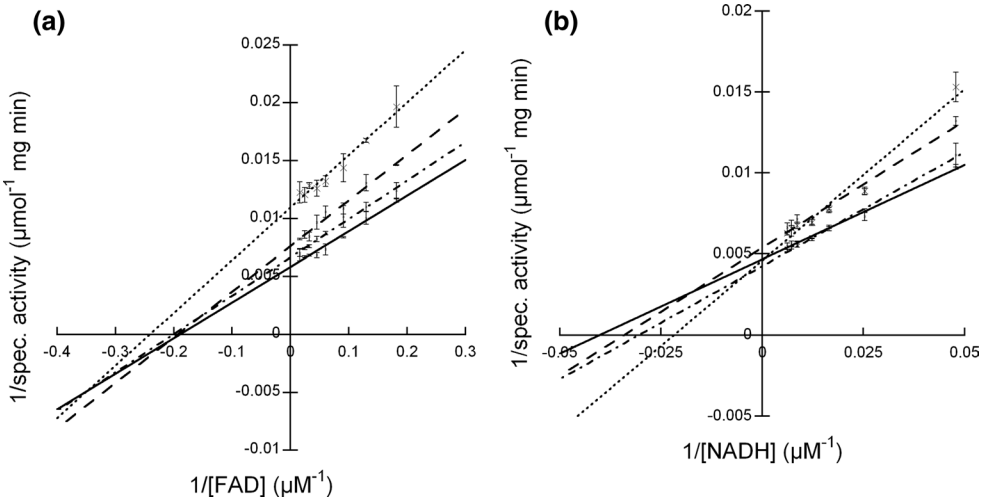


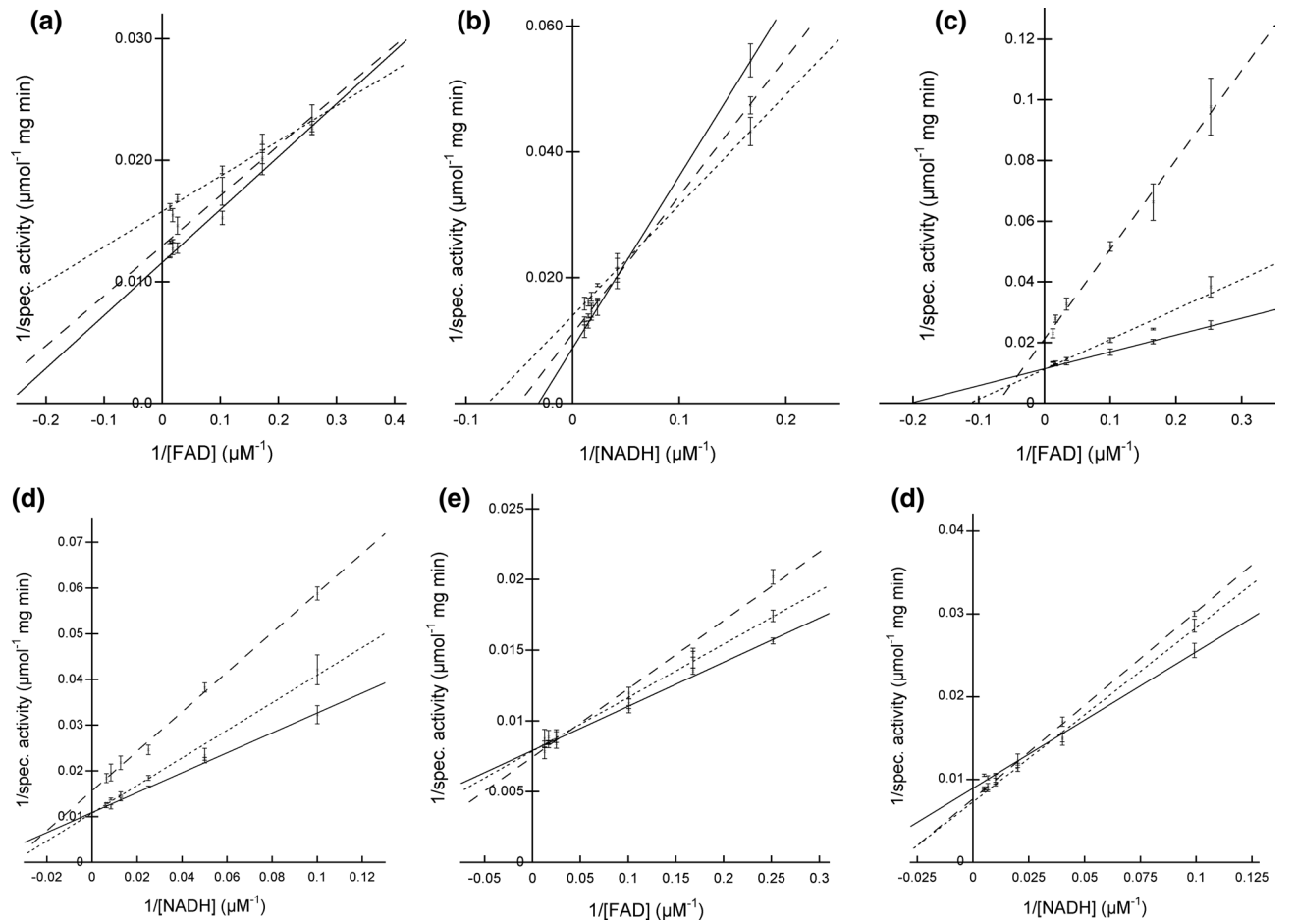


**Fig. 5** Lineweaver–Burk diagrams with **a** four different fixed NADH concentrations [161 (*solid line*), 115 (*dashed-dotted*), 77 (*dashed*), and 39 (*dotted*) µM] and varying FAD concentrations and **b** four different fixed FAD concentrations [82 (*solid line*), 51 (*dashed-dotted*), 36 (*dashed*), and 20 (*dotted*) µM] and varying NADH concentrations. *Error bars* indicate the standard deviation of three independent assays

**Fig. 6** Inhibition studies with SMOB-ADP1. Double-reciprocal plots of the initial velocity as a function of **a** NADH concentration and **b** FAD concentration, respectively, using two different $NAD^+$ concentrations (*full line* 0 mM, *dashed line* 0.83 mM, and *dotted line* 1.7 mM NAD). **c**, **d** Using lumichrome (*full line* 0 mM, *dotted line* 0.02 mM, and *dashed line* 0.06 mM) as analog of FAD. **e**, **f** Using AMP (*full line* 0 mM, *dotted line* 1.9 mM, and *dashed line* 3.7 mM) as dead-end inhibitor

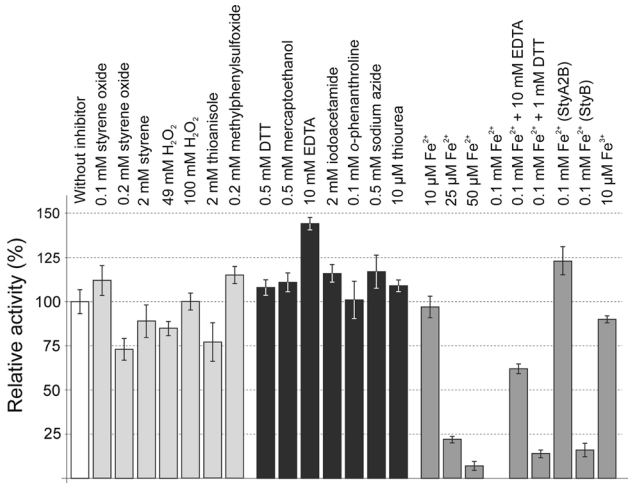


**Fig. 7** Results of an inhibition study of $His_{10}$-SMOB-ADP1 in which (*bars* in *light gray*) potential substrates and (by-) products of the corresponding monooxygenase SMOA-ADP1 (*bars* in *black*) alkylating-, reducing-, and chelating agents, and (*bars* in *dark gray*) ferrous and ferric iron were tested. Specific activities are expressed relative to the untreated enzyme (100 %), and in case of $Fe^{2+}$ effects on homologous proteins StyA2B of *R. opacus* 1CP and StyB of *Pseudomonas* sp. VLB 120 are given

A remarkable effect of the product $NAD^+$ on $His_{10}$-SMOB-ADP1 was noticed during product inhibition studies when the standard enzyme assay (25.5 µM FAD, 132 µM NADH) was incubated with concentrations exceeding 3–4 mM. Under these conditions, the mixed noncompetitive inhibition switched to a complete irreversible inhibition. SMOB-ADP1-activity could not be restored by diluting the enzyme assay and thereby lowering the $NAD^+$ concentration. This behavior was found to be highly reproducible. But due to the lack of similar results for other enzymes, we can give no hypothesis on the mechanism of inactivation.

## FAD exhibits quenched fluorescence when binding to $His_{10}$-SMOB-ADP1

The interaction of flavoproteins with their flavin cosubstrates as well as indications on the flavin-binding site can be studied by fluorescence measurements. For that purpose, fluorescence of oxidized FAD in presence and absence of SMOB-ADP1 apoenzyme was determined (Fig. 8) using an excitation wavelength of 450 nm. The intensity of the recorded fluorescence emission spectrum (maximum fluorescence at 529 ± 1 nm) was significantly quenched (about 45 % reduction) when the assay contained additionally the reductase $His_{10}$-SMOB-ADP1 in a concentration similar to the flavin concentration (Fig. 8). A similar quenching of FAD caused by binding to flavin reductases was reported earlier (Lee and Zhao 2007; Chakraborty et al. 2010). However, the related StyB from *Pseudomonas* sp. VLB120 showed a converse behavior (Otto et al. 2004) since the fluorescence of FAD-StyB was significant increased in comparison to that of free FAD.

FAD fluorescence strongly depends on molecule conformation. A reduction of the distance between the isoalloxazine ring and the adenine ring which is the case in the stacked-type conformation is associated with a decrease in fluorescence (Barrio et al. 1973). Thus, the behavior of FAD in presence of $His_{10}$-SMOB-ADP1 might indicate a preference of this stacked form and thus a shift of equilibrium between stacked- and unstacked conformation, observed in aqueous solution. However, since other interactions of the fluorophore may also cause fluorescence shifts, additional techniques are necessary to enlighten the exact binding mode of FAD to SMOB-ADP1.

However, in comparison to the related proteins StyB (Otto et al. 2004), PheA2 (van den Heuvel et al. 2004), and VlmR of *Streptomyces viridifaciens* (Parry and Li 1997), the fluorescence study provides a first hint on the mobility of the flavin in the active site. In the latter cases, the measured fluorescence signal increased for protein-FAD compared to free FAD. That clearly indicates FAD is tightly binding in a more open conformation to the protein and its mobility is significantly decreased. The binding affinity of FAD to respective proteins was shown via kinetic as well as structural studies and fits to drawn hypotheses (van den Heuvel et al. 2004; Morrison et al. 2013). So the stretched FAD molecule retains longer in a nonstacked form and therefore appears more fluorescent in respective protein environment. On the other hand, it means FAD is probably less tightly interacting with SMOB-ADP1 of strain ADP1. And somehow, this protein seems to stabilize or induce a more stacked FAD conformation and thus yields a significantly quenched fluorescence signal.

## SMOB-ADP1 has a similar dissociation constant for FAD like other NADH:flavin-dependent oxidoreductases

The dissociation constant $K_d$ for FAD was determined by the titration of a FAD stock solution to buffer containing $His_{10}$-SMOB-ADP1.

The measured fluorescence signals were fitted using the quadratic Eq. 1, and a $K_d$(FAD) of 1.82 ± 0.02 µM at 25 °C could be calculated (Fig. 9). This dissociation constant is similar to the recently published $K_d$ values of NADH:flavin-dependent oxidoreductases of styrene monooxygenases. In particular, these are StyB of *Pseudomonas* sp. strain VLB120, $K_d$(FAD) = 2.3 ± 0.3 µM (Otto et al. 2004), SMOB of *P. putida* S12, $K_d$(FAD) = 1.15 ± 0.14 µM (Morrison et al. 2013), and the oxidoreductase part of StyA2B (assuming one binding site for FAD) of *R. opacus* 1CP,

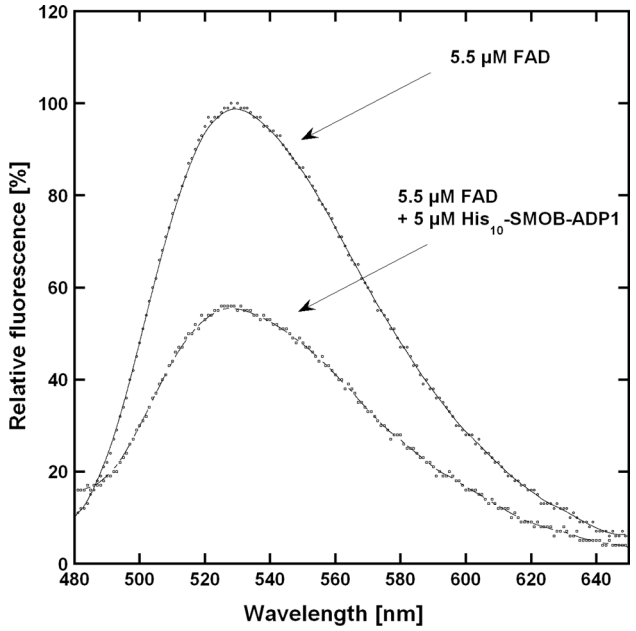


**Fig. 8** Fluorescence emission spectra of FAD in the absence and presence of $His_{10}$-SMOB-ADP1 using an excitation wavelength of 450 nm. Each point represents the duplicate determination of two individual samples

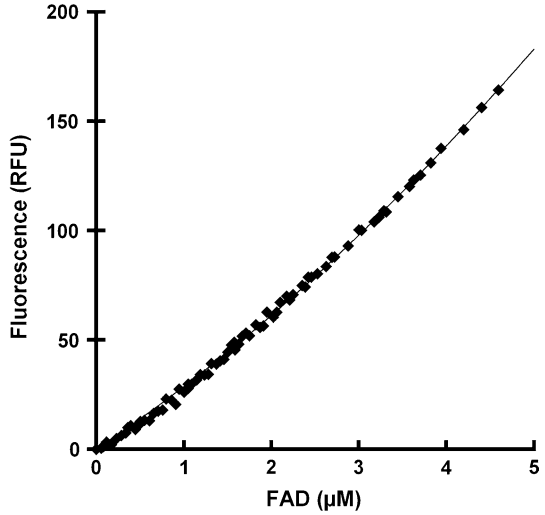


**Fig. 9** Titration of FAD to a $His_{10}$-SMOB-ADP1-containing buffer. Relative fluorescence emission was measured and the start value normalized to 0. Determinants are given in relative fluorescence units (RFUs). The fitting of the curve through the data points was calculated by employing Eq. 1, where $[SMOB\text{-}ADP1]_{total}$ was set to 3.9 µM, $\varepsilon_1$ to 57.5, and $\varepsilon_2$ to 12.4. The quadratic fit resulted in an estimation for $K_d$(FAD) of 1.82 ± 0.02 µM. Every data point consists of three measurements, and the fit as well as parameters were obtained from iterative fitting approaches. The slope of the linear part above 2.5 µM FAD is consistent with values obtained from free, oxidized FAD titration experiments (not shown)

$K_d$(FAD) = 5.05 ± 0.52 µM (Tischler et al. 2010). Also, the recently investigated NADH:flavin-dependent oxidoreductase HpaC of *Pseudomonas aeruginosa*, involved in the degradation of *p*-hydroxyphenylacetate, and the flavin reductase VlmR of *S. viridifaciens*, required by the isobutylamine *N*-hydroxylase for the oxidation of isobutylamine, exhibit a dissociation constant for FAD of 3 µM at 3 °C (Chakraborty et al. 2010) and 0.70 ± 0.05 µM (Parry and Li 1997), respectively.

In contrast, PheA2 of *G. thermoglucosidasius* A7, the oxidoreductase part of a phenol hydroxylase two-component system, shows with 9.8 ± 0.2 nM a much lower $K_d$ for FAD (van den Heuvel et al. 2004), indicating a much lower dissociation of FAD from the enzyme.

The quenching of the FAD fluorescence signal by $His_{10}$-SMOB-ADP1 was observed also in this experiment (Fig. 9). The titration of FAD in buffer without $His_{10}$-SMOB-ADP1 resulted in a steeper slope and then the observed slope when FAD was titrated to buffer containing $His_{10}$-SMOB-ADP1

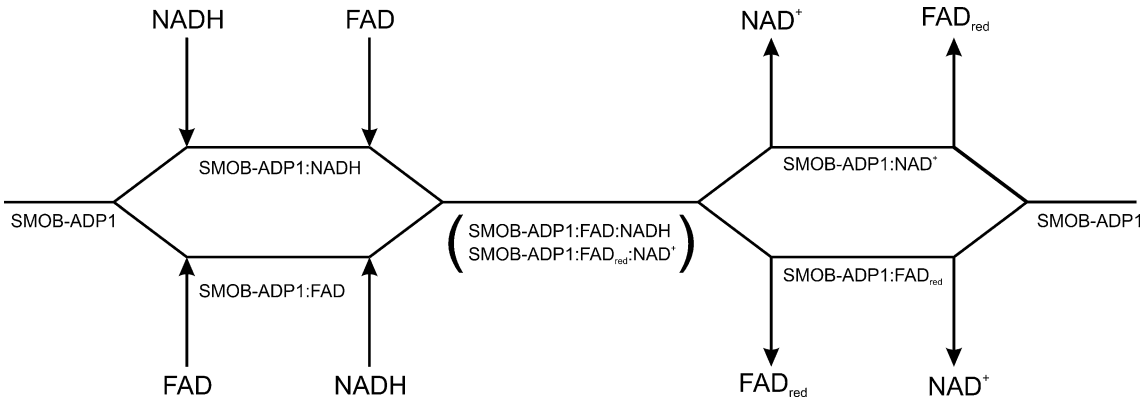


**Fig. 10** Proposed random sequential enzyme mechanism of SMOB-ADP1 of *A. baylyi* ADP1

## Conclusions

In this publication, we could verify that the gene product of *smoB*-ADP1 of *A. baylyi* ADP1 is indeed a flavin oxidoreductase, which strictly uses NADH but not NADPH as an electron donor. The results of protein sequence analysis indicate that SMOB-ADP1 belongs to the Class-I reductases and to the HpaC-like subfamily since the conserved motif GDH is present in this protein. On the other side, SMOB-ADP1 of *A. baylyi* ADP1 could be classified as FRD-II protein based on its biochemical properties, according to the review of Tu (2001). However, it is almost inevitable that a more consistent classification for flavin reductases would be helpful. By inhibition studies with analogs of FAD and NADH as well as dead-end inhibitors, strong evidences emerged that the enzymatic reaction follows a sequential random mechanism (Fig. 10). Hence, no bound flavin molecule is required for the reaction. The phylogenetic dendrogram could suggest that SMOB-ADP1 shares the same ancestor with the reported fused monooxygenases of *R. opacus* 1CP StyA2B. In contrast, biochemical and phylogenetic data indicate no close relationship of SMOB-ADP1 of strain ADP1 to StyB of *Pseudomonas*.

Flavin reductases play an important role in a variety of enzymatic redox reactions as they provide the essential dihydroflavin, e.g., for flavin-dependent monooxygenases. Likewise, these enzymes are of potential biotechnological relevance. Due to the exponential increase of sequenced genomes, availability of new representatives is not limited by the number of automatically annotated flavin reductases but rather by their kinetic and biochemical properties. It would be therefore highly desirable to reliably predict substrate preferences, necessity of bound flavin, and enzymatic reaction mechanism. Although this is already possible to some extent, further investigations and discoveries are necessary to consolidate the linkage between prediction and observed properties, what is called functional annotation.

**Acknowledgments** The project was financed by the Saxon Ministry for Environment, Agriculture, and Geology (LfULG-1771508003). Dirk Tischler was supported by the European Social Fund and the Saxon Government (GETGEOWEB: 100101363). We are grateful to Adrie Westphal for advice during fluorescence measurements.

## References

Altschul SF, Gish W, Miller W, Myers EW, Lipman DJ (1990) Basic local alignment search tool. J Mol Biol 215:403–410. doi:10.1016/S0022-2836(05)80360-2

Barrio JR, Tolman GL, Leonard NJ, Spencer RD, Weber G (1973) Flavin 1, *N*6-ethenoadenine dinucleotide: dynamic and static quenching of fluorescence. Proc Nat Acad Sci. 70:941–943. doi:10.1073/pnas.70.3.941

Beltrametti F, Marconi AM, Bestetti G, Colombo C, Galli E, Ruzzi M, Zennaro E (1997) Sequencing and functional analysis of styrene catabolism genes from *Pseudomonas fluorescens* ST. Appl Environ Microbiol 63:2232–2239

Bradford MM (1976) A rapid and sensitive method for the quantitation of microgram quantities of protein utilizing the principle of protein-dye binding. Anal Biochem 72:248–254. doi:10.1016/0003-2697(76)90527-3

Chaiyen P, Suadee C, Wilairat P (2001) A novel two-protein component flavoprotein hydroxylase. Eur J Biochem 268:5550–5561. doi:10.1046/j.1432-1033.2001.02490.x

Chakraborty S, Ortiz-Maldonado M, Entsch B, Ballou DP (2010) Studies on the mechanism of p-hydroxyphenylacetate 3-hydroxylase from *Pseudomonas aeruginosa*: a system composed of a small flavin reductase and a large flavin-dependent oxygenase. Biochemistry 49:372–385. doi:10.1021/bi901454u

Covès J, Nivière V, Eschenbrenner M, Fontecave M (1993) NADPH-sulfite reductase from *Escherichia coli*. A flavin reductase participating in the generation of the free radical of ribonucleotide reductase. J Biol Chem 268:18604–18609. doi:10.1128/JB.01050-07

Felsenstein J (1989) PHYLIP—Phylogeny Inference Package (Version 3.2). Cladistics 5:164–166

Ferreira MI, Iida T, Hasan SA, Nakamura K, Fraaije MW, Janssen DB, Kudo T (2009) Analysis of two gene clusters involved in the degradation of 4-fluorophenol by *Arthrobacter* sp. strain IF1. Appl Environ Microbiol 75:7767–7773. doi:10.1128/AEM.00171-09

Fromm HJ (1979) Summary of kinetic reaction mechanisms. Methods Enzymol 63:42–53

Galan B, Díaz E, Prieto MA, García JL (2000) Functional analysis of the small component of the 4-hydroxyphenylacetate 3-monooxygenase of *Escherichia coli* W: a prototype of a new flavin:NAD(P)H reductase subfamily. J Bacteriol 182:627–636. doi:10.1128/JB.182.3.627-636.2000

Gibello A, Suarez M, Allende JL, Martin M (1997) Molecular cloning and analysis of the genes encoding the 4-hydroxyphenylacetate hydroxylase from *Klebsiella pneumoniae*. Arch Microbiol 167:160–166. doi:10.1007/s002030050429

Gisi MR, Xun L (2003) Characterization of chlorophenol 4-monooxygenase (TftD) and NADH:flavin adenine dinucleotide oxidoreductase (TftC) of *Burkholderia cepacia* AC1100. J Bacteriol 185:2786–2792. doi:10.1128/JB.185.9.2786-2792.2003

Gouy M, Guindon S, Gascuel O (2010) SeaView version 4: a multiplatform graphical user interface for sequence alignment and phylogenetic tree building. Mol Biol Evol 27:221–224. doi:10.1093/molbev/msp259

Hartmans S, van der Werf MJ, de Bont JA (1990) Bacterial degradation of styrene involving a novel flavin adenine dinucleotide-dependent styrene monooxygenase. Appl Environ Microbiol 56:1347–1351

Hollmann F, Lin P-C, Witholt B, Schmid A (2003) Stereospecific biocatalytic epoxidation: the first example of direct regeneration of a FAD-dependent monooxygenase for catalysis. J Am Chem Soc 125:8209–8217. doi:10.1021/ja034119u

Kantz A, Gassner GT (2011) Nature of the reaction intermediates in the flavin adenine dinucleotide-dependent epoxidation mechanism of styrene monooxygenase. Biochemistry 50:523–532. doi:10.1021/bi101328r

Kantz A, Chin F, Nallamothu N, Nguyen T, Gassner GT (2005) Mechanism of flavin transfer and oxygen activation by the two-component flavoenzyme styrene monooxygenase. Arch Biochem Biophys 442:102–116. doi:10.1016/j.abb.2005.07.020

Kirchner U, Westphal AH, Müller R, van Berkel WJH (2003) Phenol hydroxylase from *Bacillus thermoglucosidasius* A7, a two-protein

component monooxygenase with a dual role for FAD. J Biol Chem 278:47545–47553. doi:10.1074/jbc.M307397200

Lee J-K, Zhao H (2007) Identification and characterization of the flavin:NADH reductase (PrnF) involved in a novel two-component arylamine oxygenase. J Bacteriol 189:8556–8563. doi:10.1128/JB.01050-07

Lei B, Tu S-C (1998) Mechanism of reduced flavin transfer from *Vibrio harveyi* NADPH-FMN oxidoreductase to luciferase. Biochemistry 37:14623–14629. doi:10.1021/bi981841+

Lei B, Liu M, Huang S, Tu S-C (1994) *Vibrio harveyi* NADPH-flavin oxidoreductase: cloning, sequencing and overexpression of the gene and purification and characterization of the cloned enzyme. J Bacteriol 176:3552–3558

Lin H, Qiao J, Liu Y, Wu Z-L (2010) Styrene monooxygenase from *Pseudomonas* sp. LQ26 catalyzes the asymmetric epoxidation of both conjugated and unconjugated alkenes. J Mol Catal B Enzym 67:236–241. doi:10.1016/j.molcatb.2010.08.012

Massey V (1994) Activation of molecular oxygen by flavins and flavoproteins. J Biol Chem 269:22459–22462

Metzgar D, Bacher JM, Pezo V, Reader J, Döring V, Schimmel P, Marlière P, De Crécy-Lagard V (2004) *Acinetobacter* sp. ADP1: an ideal model organism for genetic analysis and genome engineering. Nucleic Acids Res 32:5780–5790. doi:10.1093/nar/gkh881

Montersino S, Tischler D, Gassner GT, van Berkel WJH (2011) Catalytic and structural features of flavoprotein hydroxylases and epoxidases. Adv Synth Catal 353:2301–2319. doi:10.1002/adsc.201100384

Morrison E, Kantz A, Gassner GT, Sazinsky MH (2013) Structure and mechanism of styrene monooxygenase reductase: new insight into the FAD-transfer reaction. Biochemistry 52:6063–6075. doi:10.1021/bi400763h

O'Leary ND, O'Connor KE, Duetz W, Dobson ADW (2001) Transcriptional regulation of styrene degradation in *Pseudomonas putida* CA-3. Microbiology 147:973–979

Otto K, Hofstetter K, Röthlisberger M, Witholt B, Schmid A (2004) Biochemical characterization of StyAB from *Pseudomonas* sp. strain VLB120 as a two-component flavin-diffusible monooxygenase. J Bacteriol 186:5292–5302. doi:10.1128/JB.186.16.5292-5302.2004

Panke S, Witholt B, Schmid A, Wubbolts MG (1998) Towards a biocatalyst for (*S*)-styrene oxide production: characterization of the styrene degradation pathway of *Pseudomonas* sp. strain VLB120. Appl Environ Microbiol 64:2032–2043

Parry RJ, Li W (1997) An NADPH:FAD oxidoreductase from the valanimycin producer, *Streptomyces viridifaciens*. Cloning, analysis, and overexpression. J Biol Chem 272:23303–23311. doi:10.1074/jbc.272.37.23303

Prieto MA, Garcia JL (1994) Molecular characterization of 4-hydroxyphenylacetate 3-hydroxylase of *Escherichia coli*. A two-protein component enzyme. J Biol Chem 269:22823–22829

Riedel A, Mehnert M, Heine T, Rathsack P, Kaschabek SR, Schlömann M, Tischler D (2013) GDCh - Wissenschaftsforum Chemie 2013, BIO 011. Darmstadt

Rudolph FB (1979) Product inhibition and abortive complex formation. Methods Enzymol 63:411–436

Russell TR, Tu S-C (2004) *Aminobacter aminovorans* NADH:flavin oxidoreductase His140: a highly conserved residue critical for NADH binding and utilization. Biochemistry 43:12887–12893. doi:10.1021/bi048499n

Russell TR, Demeler B, Tu S-C (2004) Kinetic mechanism and quaternary structure of *Aminobacter aminovorans* NADH:flavin oxidoreductase: an unusual flavin reductase with bound flavin. Biochemistry 43:1580–1590. doi:10.1021/bi035578a

Saa L, Jaureguibeitia A, Largo E, Llama MJ, Serra JL (2010) Cloning, purification and characterization of two components of phenol hydroxylase from *Rhodococcus erythropolis* UPV-1. Appl Microbiol Biotechnol 86:201–211. doi:10.1007/s00253-009-2251-x

Sambrook J, Fritsch EF, Maniatis T (2001) Molecular cloning: a laboratory manual, 3rd edn. Cold Spring Harbor Laboratory Press, Plainview

Takeo M, Yasukawa T, Abe Y, Niihara S, Maeda Y, Negoro S (2008) Mechanism of 4-nitrophenol oxidation in *Rhodococcus* sp. Strain PN1: characterization of the two-component 4-nitrophenol hydroxylase and regulation of its expression. J Bacteriol 190:7367–7374. doi:10.1128/JB.00742-08

Thiel M, Kaschabek S, Gröning J, Mau M, Schlömann M (2005) Two unusual chlorocatechol catabolic gene clusters in *Sphingomonas* sp. TFD44. Arch Microbiol 183:80–94. doi:10.1007/s00203-004-0748-3

Thompson JD, Gibson TJ, Plewniak F, Jeanmougin F, Higgins DG (1997) The CLUSTAL_X windows interface: flexible strategies for multiple sequence alignment aided by quality analysis tools. Nucleic Acids Res 25:4876–4882. doi:10.1093/nar/25.24.4876

Thotsaporn K, Sucharitakul J, Wongratana J, Suadee C, Chaiyen P (2004) Cloning and expression of p-hydroxyphenylacetate 3-hydroxylase from *Acinetobacter baumannii*: evidence of the divergence of enzymes in the class of two-protein component aromatic hydroxylases. Biochim Biophys Acta 1680:60–66. doi:10.1016/j.bbaexp.2004.08.003

Tischler D, Kaschabek SR (2012) Microbial degradation of xenobiotics. In: Singh SN (ed) Environmental science and engineering. Springer, Heidelberg, pp 67–99

Tischler D, Eulberg D, Lakner S, Kaschabek SR, van Berkel WJH, Schlömann M (2009) Identification of a novel self-sufficient styrene monooxygenase from *Rhodococcus opacus* 1CP. J Bacteriol 191:4996–5009. doi:10.1128/JB.00307-09

Tischler D, Kermer R, Gröning JAD, Kaschabek SR, van Berkel WJH, Schlömann M (2010) StyA1 and StyA2B from *Rhodococcus opacus* 1CP: a multifunctional styrene monooxygenase system. J Bacteriol 192:5220–5227. doi:10.1128/JB.00723-10

Tischler D, Gröning JAD, Kaschabek SR, Schlömann M (2012) One-component styrene monooxygenases: an evolutionary view on a rare class of flavoproteins. Appl Biochem Biotechnol 167:931–944. doi:10.1007/s12010-012-9659-y

Tiwari MK, Singh RK, Lee J-K, Zhao H (2012) Mechanistic studies on the flavin:NADH reductase (PrnF) from *Pseudomonas fluorescens* involved in arylamine oxygenation. Bioorg Med Chem Lett 22:1344–1347. doi:10.1016/j.bmcl.2011.12.078

Toda H, Itoh N (2012) Isolation and characterization of styrene metabolism genes from styrene-assimilating soil bacteria *Rhodococcus* sp. ST-5 and ST-10. J Biosci Bioeng 113:12–19. doi:10.1016/j.jbiosc.2011.08.028

Tu S-C (2001) Reduced flavin: donor and acceptor enzymes and mechanisms of channeling. Antioxid Redox Sign 3:881–897. doi:10.1089/15230860152665046

Ukaegbu UE, Kantz A, Beaton M, Gassner GT, Rosenzweig AC (2010) Structure and ligand binding properties of the epoxidase component of styrene monooxygenase. Biochemistry 49:1678–1688. doi:10.1021/bi901693u

van Berkel WJH, Kamerbeek NM, Fraaije MW (2006) Flavoprotein monooxygenases, a diverse class of oxidative biocatalysts. J Biotechnol 124:670–689. doi:10.1016/j.jbiotec.2006.03.044

van den Heuvel RHH, Westphal AH, Heck AJR, Walsh MA, Rovida S, van Berkel WJH, Mattevi A (2004) Structural studies on flavin reductase PheA2 reveal binding of NAD in an unusual folded conformation and support novel mechanism of action. J Biol Chem 279:12860–12867. doi:10.1074/jbc.M313765200

van Hellemond EW, van Dijk M, Heuts DPHM, Janssen DB, Fraaije MW (2008) Discovery and characterization of a putrescine oxidase from *Rhodococcus erythropolis* NCIMB 11540. Appl Microbiol Biotechnol 78:455–463. doi:10.1007/s00253-007-1310-4

van Lanen SG, Lin S, Horsman GP, Shen B (2009) Characterization of SgcE6, the flavin reductase component supporting FAD-dependent halogenation and hydroxylation in the biosynthesis of the enediyne antitumor antibiotic C-1027. FEMS Microbiol Lett 300:237–241. doi:10.1111/j.1574-6968.2009.01802.x

Velasco A, Alonso S, García JL, Perera J, Díaz E (1998) Genetic and functional analysis of the styrene catabolic cluster of *Pseudomonas* sp. strain Y2. J Bacteriol 180:1063–1071